

## GdN thin film: Chern insulating state on square lattice

Zhi Li,<sup>1</sup> Jinwoong Kim,<sup>2</sup> Nicholas Kioussis,<sup>2</sup> Shu-Yu Ning,<sup>1</sup> Haibin Su,<sup>3,4,\*</sup> Toshiaki Iitaka,<sup>5</sup> Takami Tohyama,<sup>6</sup> Xinyu Yang,<sup>1</sup> and Jiu-Xing Zhang<sup>1,†</sup>

<sup>1</sup>*School of Materials Science and Engineering, Hefei University of Technology, Hefei 230009, Anhui, China*

<sup>2</sup>*Department of Physics, California State University Northridge, Northridge, California 91330-8268, USA*

<sup>3</sup>*Division of Materials Science, Nanyang Technological University, 50 Nanyang Avenue, 639798 Singapore*

<sup>4</sup>*Institute of Advanced Studies, Nanyang Technological University, 60 Nanyang View, 639673 Singapore*

<sup>5</sup>*Computational Astrophysics Laboratory, RIKEN, 2-1 Hirosawa, Wako, Saitama 351-0198, Japan*

<sup>6</sup>*Department of Applied Physics, Tokyo University of Science, Katsushika, Tokyo 125-8585, Japan*

(Received 4 June 2015; published 10 November 2015)

Using first-principles calculations, we predict a Chern insulating phase in thin films of the ferromagnetic semimetal GdN. In contrast to previously proposed Chern insulator candidates, which mostly rely on honeycomb lattices, this system affords a great chance to realize the quantum anomalous Hall effect on a square lattice without either a magnetic substrate or transition metal doping, making synthesis easier. The band inversion between the  $5d$  orbitals of Gd and  $2p$  orbitals of N is verified by first-principles calculations based on density functional theory, and the band gap can be as large as 100 meV within the GdN trilayer. With a further increase of film thickness, the band gap tends to close and the metallic bulk property becomes obvious.

DOI: [10.1103/PhysRevB.92.201303](https://doi.org/10.1103/PhysRevB.92.201303)

PACS number(s): 73.43.-f, 71.20.Mq, 73.61.Ey

The topological insulator (TI) as a exotic quantum state has been experimentally realized in several materials with strong spin-orbit coupling (SOC) [1–3]. The Chern insulator, as a material which can realize the quantum anomalous Hall effect (QAHE), also has attracted lots of research interest. The QAHE, i.e., a quantum Hall effect without an external magnetic field, proposed by Haldane on a hexagonal lattice [4], recently has been realized in a chromium-doped  $(\text{Bi,Sb})_2\text{Te}_3$  thin film [5–7]. However, the chromium-doped  $(\text{Bi,Sb})_2\text{Te}_3$  thin film exhibits ferromagnetic (FM) spin order only below 15 K, and the transverse conductivity  $\sigma_{xy}$  becomes quantized to better than 1/10 only below 400 mK. In addition, the QAHE also is proposed in magnetic quantum wells (QWs) [8–10], honeycomb materials with induced ferromagnetism (FM) [11–17], and magnetically doped thin-film topological crystalline insulators [18]. However, for the magnetic quantum well and honeycomb materials, the band gap usually is very small, and all the proposed materials are fairly difficult to fabricate. Recently, a Chern insulator with a square lattice has also been proposed in an interface of  $\text{CrO}_2$  and  $\text{TiO}_2$  [19], double-perovskite monolayers [20], and magnetic rocksalt interfaces [21,22]. The QAHE can persist up to room temperature in a band gap of the  $\text{EuO}/\text{GdN}$  multilayer that is even as large as 0.1 eV [22]. The QW structure of the Weyl semimetal (WSM) affords another simple platform to realize the QAHE [23]. The WSM is a type of topological matter with pairs of separated Weyl points or band crossings. The Weyl points can only appear when the spin-doublet degeneracy of each band is removed by broken time-reversal symmetry or spatial inversion symmetry [24]. For a realization of the QAHE, we can consider a thin film of WSM with broken time-reversal symmetry resulting from FM spin order. The Weyl semimetal

phase in a three-dimensional (3D) structure of stacked FM multilayers of TIs was also proposed by Burkov *et al.* [25].

In this Rapid Communication, we propose the realization of QAHE in a GdN [001] thin film, which has a relatively large band gap for working at room temperature. Bulk GdN with a rocksalt structure is known as a ferromagnetic half metal with a Curie temperature  $T_c \sim 58$  K [26–32]. It was intensively studied in the 1960's and 1990's due to its potential application in spintronics devices. By first-principles calculations based on density functional theory (DFT) and tight-binding (TB) model calculations, we predict that the band crossing in the FM GdN bulk is unavoidable even if spin-orbit coupling (SOC) is included in the first-principles calculation, and the band crossing between  $d$ - $p$  orbitals in GdN bulk is protected by fourfold rotation symmetry. The  $d$ - $p$  band inversion or crossing has been discovered in several materials, such as the noncentrosymmetric superconductor  $\text{PbTaSe}_2$  [33], the non-Kondo-like topological insulator  $\text{YbB}_6$  [34,35], the topological insulator  $\text{LaX}$  ( $X = \text{P, As, Sb, Bi}$ ), the Weyl semimetal  $\text{TaAs}$  [36], and the topological semimetal  $\text{LaN}$  [37]. We also predict a FM GdN thin film as a Chern insulator with  $d$ - $p$  band inversion on a square lattice. Since time-reversal symmetry is broken by the FM spin order of Gd  $4f$  electrons, no magnetic doping or substrate is required. The  $d$ - $p$  band inversion starts in the free-standing GdN bilayer, and the band gap has a maximal value  $\sim 100$  meV in the trilayer. With an increase of thickness of the thin film, the metallic bulk character will become obvious, viz., the band gap will approach to zero.

The DFT calculations employed the all-electron, full-potential linearized augmented plane wave (FP-LAPW) method with a generalized gradient approximation plus Hubbard  $U$  (GGA +  $U$ ) implemented in the WIEN2K code [38]. The SOC was included in the self-consistent calculations. We have used the experimental value  $a_0 = 4.97$  Å for the lattice parameter,

\*hbsu@ntu.edu.sg

†zjiuxing@hfut.edu.cn

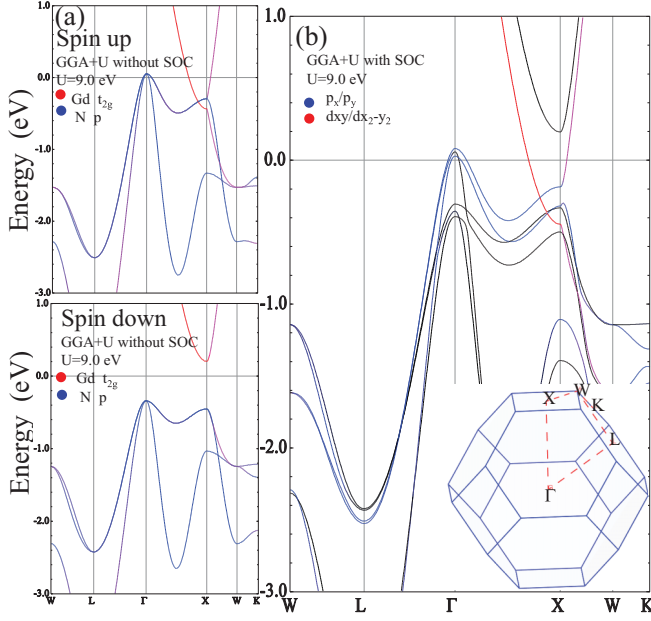


FIG. 1. (Color online) The band structures of FM GdN bulk by GGA +  $U_{\text{eff}}$  calculation (a) without SOC and (b) with SOC. In (a), the Gd  $t_{2g}$  orbitals are in red, and N  $p$  orbitals are in blue. In (b), the Gd  $d_{xy}/d_{x^2-y^2}$  orbitals are in red, the N  $p_x/p_y$  orbitals are in blue, and all the spin-down bands are in black.

and the effective Hubbard  $U_{\text{eff}}$  for the Gd  $4f$  orbitals is set to be 9.0 eV, determined by the occupied Gd  $4f$  levels in GdP by optical experiments [29].

**Bulk GdN.** GdN is a unique FM material in the gadolinium mononictides, and its lattice-dependent Curie temperature can be up to 70 K. The electronic structure of FM bulk GdN calculated by GGA +  $U$  without SOC is shown in Fig. 1(a). With a deeply buried  $4f$  electron resulting from strong electronic correlation and a FM Zeeman field, the Gd  $d_{xy}$  and N  $p$  orbitals make the main contribution to the electronic structure near the Fermi level. It reveals that the FM bulk GdN is half metallic, i.e., a metallic character within spin-up bands and an insulating character within spin-down bands. Of interest, there is a band crossing along the  $\Gamma \rightarrow X$  direction between the Gd  $d_{xy}$  orbitals and the N  $p_x$  ( $p_y$ ) orbitals. This  $d_{xy}/p_x$  ( $p_y$ ) band crossing is protected by the  $M_{zx}$  ( $M_{yz}$ ) mirror plane, which maps  $y(x)$  to  $-y(-x)$ . In the Brillouin zone (BZ) [shown in the inset of Fig. 1(b)], bands on the  $k_y = 0$  and  $k_x = 0$  planes can be labeled by their eigenvalues of  $M_{zx}$  and  $M_{yz}$ , respectively. Obviously, the  $p_x$  ( $p_y$ ) orbitals and  $d_{xy}$  orbitals have different  $M_{zx}$  ( $M_{yz}$ ) eigenvalues of 1 and  $-i$ , respectively, and they cannot hybridize on the  $k_y$  ( $k_x$ ) = 0 plane. Along the  $\Gamma \rightarrow X$  direction, i.e.,  $(0,0,0)$ - $(0,0,2\pi)$ , both  $p_x$  and  $p_y$  orbitals cannot hybridize with the  $d_{xy}$  orbitals. In the TIs, SOC can remove this band crossing and open a gap; the stability of the band crossing against the SOC perturbation is an important question here. The band structure of FM bulk GdN calculated by GGA +  $U$  with SOC is shown in Fig. 1(b), and it reveals that  $d_{xy}$  orbitals still cannot hybridize with the  $p_x$  and  $p_y$  orbitals to open a gap. With the spin quantization axis along the  $z$  axis, the  $p_x \pm ip_y$  orbital has a quantized orbital momentum  $\hbar$ , and it has a

definite eigenvalue of  $\mp i$  under fourfold rotation symmetry  $C_{4z}$ . However, the  $d_{xy}$  orbital has an eigenvalue of  $-1$  under  $C_{4z}$  [39]. The band crossing between the  $d/p$  orbitals still can be protected by fourfold rotation symmetry  $C_{4z}$ . Since the high-symmetry line  $\Gamma \rightarrow X$  is a  $C_{4z}$  invariant line, energy bands with a different  $C_{4z}$  eigenvalue along this line cannot hybridize with each other. So, we conclude that the  $d/p$  band crossing in FM bulk GdN is stable against SOC perturbation if the  $C_{4z}$  is not broken. We note that the bandwidth of Gd  $5d$  orbitals is strongly dependent with the lattice constant [40–44]. With a reduced lattice parameter, both the bandwidth of Gd  $5d$  and the ferromagnetism will be enhanced in strained GdN [44].

The band crossing in the FM bulk GdN can be described by a simple tight-binding model (TB) on a face-centered cubic lattice with Gd  $d = d_{xy}$  and N  $p = p_x + ip_y$ , as the basis, which can be expressed as

$$H = H_d + H_p + H_{dp},$$

$$H_d = \epsilon_d + t_d \sum_i d_i d_{i \pm \frac{e_x + e_y}{2}} + t'_d \sum_i d_i d_{i \pm \frac{e_y + e_z(x)}{2}} + \text{H.c.},$$

$$H_p = t_p \sum_i p_i p_{i \pm \frac{e_x + e_y}{2}} + t'_p \sum_i d_i d_{i \pm \frac{e_y + e_z(x)}{2}} + \text{H.c.},$$

$$H_{dp} = t_{dp} \sum_i p_i (d_{i + \frac{e_x}{2}} - i d_{i + \frac{e_y}{2}} - d_{i - \frac{e_x}{2}} + i d_{i - \frac{e_y}{2}}).$$

With Fourier transformation, the Hamiltonian reads

$$H = \sum_k \begin{pmatrix} p_k \\ d_k \end{pmatrix}^\dagger \begin{pmatrix} A(k) & V(k) \\ V(k)^\dagger & B(k) \end{pmatrix} \begin{pmatrix} p_k \\ d_k \end{pmatrix},$$

$$A(k) = 4t_p \cos \frac{k_x}{2} \cos \frac{k_y}{2} + 4t'_p \left( \cos \frac{k_y}{2} \cos \frac{k_z}{2} + \cos \frac{k_x}{2} \cos \frac{k_z}{2} \right),$$

$$B(k) = \epsilon_d + 4t_d \cos \frac{k_x}{2} \cos \frac{k_y}{2} + 4t'_d \left( \cos \frac{k_y}{2} \cos \frac{k_z}{2} + \cos \frac{k_x}{2} \cos \frac{k_z}{2} \right),$$

$$V(k) = 2t_{dp} \left( \sin \frac{k_y}{2} + i \sin \frac{k_x}{2} \right),$$

in momentum space. The  $A(k)$  and  $B(k)$  terms describe the  $d$ - and  $p$ -band dispersion without hybridization. The  $V(k)$  describes the hybridization on different momentum points. The vanishing  $d$ - $p$  hybridization along the  $(0,0,0)$ - $(0,0,\pi)$  direction is obvious, and the  $d$ - $p$  band crosses at  $k_z = 0.69\pi$ , estimated by an on-site energy  $\epsilon_d = 4.2$  eV and hopping parameters  $t_d = -0.93$  eV,  $t'_d = 0.23$  eV,  $t_p = 0.14$  eV,  $t'_p = 0.07$  eV, and  $t_{dp} = 0.93$  eV extracted from a Wannier calculation with five Gd  $d$  orbitals and three N  $p$  orbitals [45]. With these parameters, the first Chern number is  $-1$  when  $k_z$  is in  $(-\pi, -0.69\pi)$  and  $(0.69\pi, \pi]$ , and zero when  $k_z$  is in  $(-0.69\pi, 0.69\pi)$ . The calculated band structures and surface states of GdN by the TB model are provided in the Supplemental Material [46].

**Thin-film GdN.** Since the Gd  $d_{xy}$  and N  $p$  band crossing is protected by fourfold rotation symmetry  $C_{4z}$ , it is possible

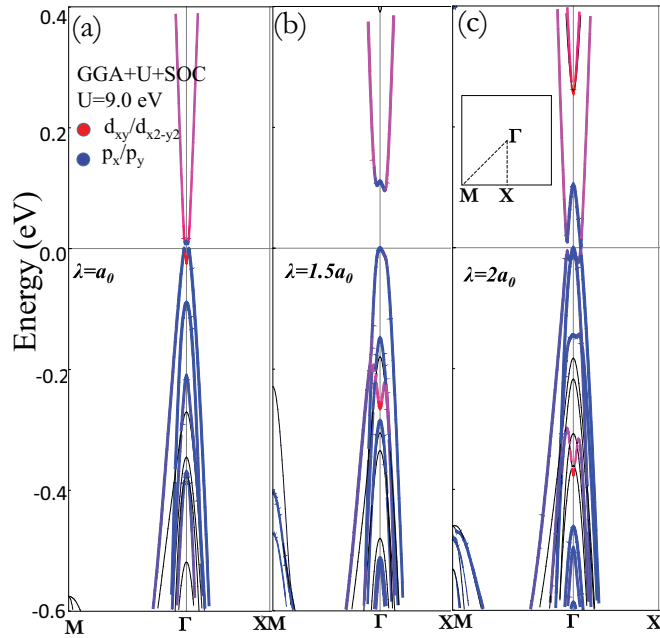


FIG. 2. (Color online) Band structures of GdN (a) (AB) bilayer, (b) (ABA) trilayer, and (c) two bilayers, calculated by GGA +  $U_{\text{eff}}$  + SOC. The weight of  $d_{x^2-y^2}$  and  $p_x, p_y$  orbitals is represented by red and blue colors. All the spin-down bands are in black.

to remove this band crossing by size confinement, i.e., eliminate the  $z$  direction. The GdN [001] thin film, which can be regarded as a stack of GdN A and B monolayers along the  $z$  direction, becomes a prospective Chern insulator candidate with a square lattice, instead of the extensively studied honeycomb lattice. With lattice vectors  $\vec{a} = \frac{a_0}{\sqrt{2}}(1, 0)$ ,  $\vec{b} = \frac{a_0}{\sqrt{2}}(0, 1)$ , the B monolayer has an offset  $(0.5, 0.5)$  relative to the A monolayer. With a vanishing interlayer hopping parameter  $t'_d = t'_p = 0$  in the TB model, the  $d_{xy}$  band always has a higher energy than the  $p$  orbitals dominating bands over the entire BZ, i.e., the monolayer of GdN should be insulating, which is consistent with our first-principles calculated result of a free-standing GdN monolayer. The calculated electronic structures of the free-standing AB bilayer (BL), ABA trilayer (TL), and four monolayers with thickness  $\lambda = a_0$ ,  $1.5a_0$ , and  $2a_0$  by first-principles calculation with GGA +  $U_{\text{eff}}$  + SOC are shown in Fig. 2. The spin-up Gd  $d$  ( $=d_{x^2-y^2}$ ) orbitals in red and N  $p$  ( $=p_x \pm ip_y$ ) orbitals in blue are hybridized near the Fermi level, and all the spin-down bands are in black. Our calculated results show that the  $d/p$  band inversion starts in the BL, though the band gap resulting from  $d-p$  hybridization is minute. However, in the TL, the band gap can increase up to 100 meV, which almost is the same as the band gap in the GdN/EuO interface [22]. Because of the enhanced bandwidth resulting from interlayer  $d-d$  and  $p-p$  hybridization, the  $d$  orbitals and  $p$  orbitals on the B layer are inverted near the center of the BZ and hybridized, and this  $d/p$  band inversion contributes  $-1$  to the Chern number. In both the GdN bilayer and trilayer, the A monolayer behaves as a normal two-dimensional (2D) insulator because there is no  $d$  band from the A layer involved in the band inversion, as shown in Fig. 2(b). This GdN trilayer can be regarded as a Chern

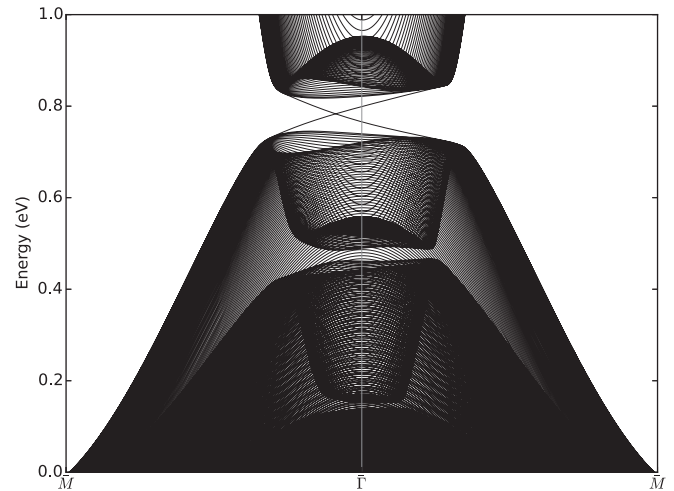


FIG. 3. Calculated tight-binding electronic structure of FM GdN in the form of a one-dimensional (1D) ribbon with  $\epsilon_d = 4.2$  eV,  $t_{pp} = 0.14$  eV,  $t_{dd} = -0.73$  eV,  $t'_{dd} = 0.23$  eV,  $t'_{pp} = 0.07$  eV,  $t_{dp} = 0.93$  eV, and  $t'_{dp} = 0.05$  eV. A pair of metallic surface states comes from the left and right terminations of the ribbon.

insulator sandwiched by an ordinary insulator layer [25]. The intralayer  $d/p$  hybridization gap is  $\sim 0.3$  eV. However, the global band gap is reduced to 100 meV because of the weaker interlayer  $d/p$  hybridization. With a further increase of thickness, more  $d/p$  band inversions tend to take place. However, the band gap is seriously reduced because of the vanishing long distant interlayer  $d/p$  hybridization, as shown in Fig. 2(c). Even though the intralayer  $d-p$  hybridization can be very strong here, the  $p$  bands from the normal insulator layers are always obstructions to obtain a large band gap. We also notice that the calculated band gap also decreases with an increase of the GdN monolayer in the EuO/GdN multilayer [22].

The electronic structure of a one-dimensional ribbon of TL is calculated by the TB model with Gd  $d_{x^2-y^2}$  orbitals and N  $p_x + ip_y$  orbitals as the basis with on-site energy  $\epsilon_d = 4.2$  eV and  $t_d = 0.73$  eV,  $t'_d = 0.23$  eV,  $t_p = 0.14$  eV, and  $t'_p = 0.07$  eV. We also include a small interlayer  $d-p$  hopping parameter  $t'_{dp} = 0.05$  eV, which is proportional to the  $(pd\pi)$  integral. The calculated electronic structure of the 1D ribbon is shown in Fig. 3, and two boundary states with opposite chirality, from the left and right ends of the ribbon, are predicted. This metallic surface state is consistent with the prediction of quantized Hall conductivity in the multilayer structure of the ferromagnetic topological insulator [25]. We also note here that we assume the spin easy axis is along the  $z$  axis in all our calculations because of the quantized orbital momentum along the  $z$  axis. In fact, the magnetocrystalline anisotropic energy of the GdN TL is very minute and less than 2 meV, so a weak external magnetic field is necessary to keep the spin lying along the  $z$  axis at finite temperature.

For the epitaxial fabrication of a [001] GdN thin film, usually a substrate is required. Here, we also calculate the electronic structure of GdN TL with six monolayers of YN. The lattice parameter of YN in a rocksalt structure is 4.88 Å,

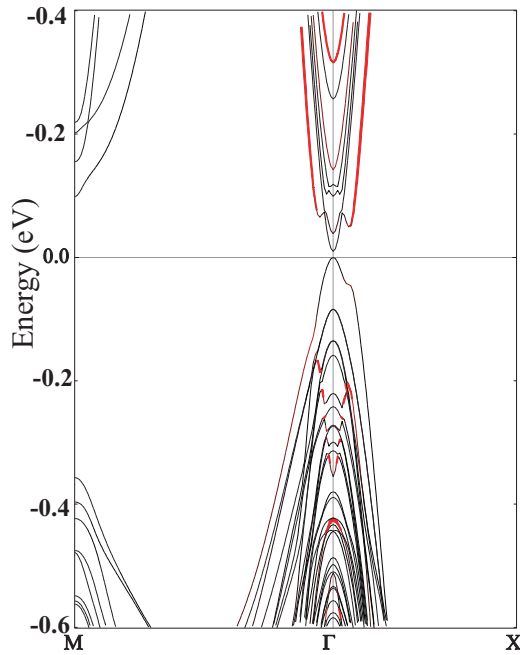


FIG. 4. (Color online) Calculated electronic structure of GdN TL on six YN monolayers by GGA +  $U_{\text{eff}}$  + SOC. The Gd  $d_{x^2-y^2}$  orbitals are in red.

which is very close to the GdN lattice parameter 4.98 Å. The electronic structure of this GdN/YN multilayer calculated by GGA +  $U_{\text{eff}}$  + SOC is shown in Fig. 4 with Gd  $d_{x^2-y^2}$  orbitals in red, and the  $d/p$  band inversion is reproduced. However, the calculated band gap is about 20 meV, indicating a better substrate should be explored in future work.

In summary, we predict a Weyl semimetal phase and a Chern insulator phase in FM bulk and thin-film GdN, respectively. In the bulk GdN, the  $d-p$  band crossing is protected by fourfold rotation symmetry  $C_{4z}$ , and it is robust against SOC. A Chern insulating state on a square lattice is predicted on the [001] thin-film GdN, and its multilayer structure affords a concrete realization of a 3D Weyl semimetal phase. The maximal band gap is  $\sim 100$  meV, which is present in the free-standing GdN TL with a single  $d/p$  band inversion. With an increasing thickness of the thin film, the band gap tends to close and a metallic bulk state will become obvious.

This work is supported by National Natural Science Foundation of China under Grant No. 51371010 and the Fundamental Research Funds for the Central Universities. The research at CSUN was supported by NSF-PREM Grant No. DMR-1205734. The authors also are grateful to J. P. Hu for useful discussions.

- [1] M. Z. Hasan and C. L. Kane, *Rev. Mod. Phys.* **82**, 3045 (2010).
- [2] X. L. Qi and S. C. Zhang, *Rev. Mod. Phys.* **83**, 1057 (2011).
- [3] Y. Ando, *J. Phys. Soc. Jpn.* **82**, 102001 (2013).
- [4] F. D. M. Haldane, *Phys. Rev. Lett.* **61**, 2015 (1988).
- [5] R. Yu, W. Zhang, H.-J. Zhang, S.-C. Zhang, X. Dai, and Z. Fang, *Science* **329**, 61 (2010).
- [6] C.-Z. Chang *et al.*, *Science* **340**, 167 (2013).
- [7] X.-F. Kou, S. T. Guo, Y. Fan, L. Pan, M. Lang, Y. Jiang, Q. Shao, T. Nie, K. Murata, J. Tang, Y. Wang, L. He, T. K. Lee, W. L. Lee, and K. L. Wang, *Phys. Rev. Lett.* **113**, 137201 (2014).
- [8] C.-X. Liu, X.-L. Qi, X. Dai, Z. Fang, and S.-C. Zhang, *Phys. Rev. Lett.* **101**, 146802 (2008).
- [9] H.-C. Hsu, X. Liu, and C.-X. Liu, *Phys. Rev. B* **88**, 085315 (2013).
- [10] H. J. Zhang, J. Wang, G. Xu, Y. Xu, and S.-C. Zhang, *Phys. Rev. Lett.* **112**, 096804 (2014).
- [11] R. Nandkishore and L. Levitov, *Phys. Rev. B* **82**, 115124 (2010).
- [12] Z. H. Qiao, S. A. Yang, W. X. Feng, W.-K. Tse, J. Ding, Y. G. Yao, J. Wang, and Q. Niu, *Phys. Rev. B* **82**, 161414(R) (2010).
- [13] M. Ezawa, *Phys. Rev. Lett.* **109**, 055502 (2012).
- [14] H. B. Zhang, C. Lazo, S. Blügel, S. Heinze, and Y. Mokrousov, *Phys. Rev. Lett.* **108**, 056802 (2012).
- [15] X.-L. Zhang, L.-F. Liu, and W.-M. Liu, *Sci. Rep.* **3**, 2908 (2013).
- [16] H. Pan, Z. S. Li, C.-C. Liu, G. B. Zhu, Z. H. Qiao, and Y. G. Yao, *Phys. Rev. Lett.* **112**, 106802 (2014).
- [17] S.-C. Wu, G. C. Shan, and B. H. Yan, *Phys. Rev. Lett.* **113**, 256401 (2014).
- [18] C. Fang, M. J. Gilbert, and B. A. Bernevig, *Phys. Rev. Lett.* **112**, 046801 (2014).
- [19] T. Cai, X. Li, F. Wang, J. Sheng, J. Feng, and C.-D. Gong, *Nano Lett.* **15**, 6434 (2015).
- [20] H. Zhang, H. Huang, K. Haule, and D. Vanderbilt, *Phys. Rev. B* **90**, 165143 (2014).
- [21] K. F. Garrity and D. Vanderbilt, *Phys. Rev. Lett.* **110**, 116802 (2013).
- [22] K. F. Garrity and D. Vanderbilt, *Phys. Rev. B* **90**, 121103(R) (2014).
- [23] G. Xu, H. M. Weng, Z. J. Wang, X. Dai, and Z. Fang, *Phys. Rev. Lett.* **107**, 186806 (2011).
- [24] X. Wan, A. M. Turner, A. Vishwanath, and S. Y. Savrasov, *Phys. Rev. B* **83**, 205101 (2011).
- [25] A. A. Burkov and L. Balents, *Phys. Rev. Lett.* **107**, 127205 (2011).
- [26] F. Hulliger, in *Handbook on the Physics and Chemistry of Rare Earths*, edited by K. A. Gschneidner, Jr. and L. R. Eyring (North-Holland, Amsterdam, 1979), Vol. 4, p. 151.
- [27] D. X. Li, Y. Haga, H. Shida, T. Suzuki, Y. S. Kwon, and G. Kido, *J. Phys.: Condens. Matter* **9**, 10777 (1997).
- [28] F. Leuenberger, A. Parge, W. Felsch, K. Fauth, and M. Hessler, *Phys. Rev. B* **72**, 014427 (2005).
- [29] C.-G. Duan, R. F. Sabirianov, W. N. Mei, P. A. Dowben, S. S. Jaswal, and E. Y. Tsymlal, *J. Phys.: Condens. Matter* **19**, 315220 (2007).
- [30] K. Senapati, T. Fix, Mary E. Vickers, M. G. Blamire, and Z. H. Barber, *Phys. Rev. B* **83**, 014403 (2011).
- [31] P. Wachter, *Results Phys.* **2**, 90 (2012).
- [32] F. Natali, B. J. Ruck, N. O. V. Planck, H. J. Trodahl, S. Granville, C. Meyer, and W. R. L. Lambrecht, *Prog. Mater. Sci.* **58**, 1316 (2013).
- [33] G. Bian *et al.*, [arXiv:1505.03069](https://arxiv.org/abs/1505.03069).



- [34] M. Neupane, S. Y. Xu, N. Alidoust, G. Bian, D. J. Kim, C. Liu, I. Belopolski, T. R. Chang, H. T. Jeng, T. Durakiewicz, H. Lin, A. Bansil, Z. Fisk, and M. Z. Hasan, *Phys. Rev. Lett.* **114**, 016403 (2015).
- [35] T.-R. Chang, T. Das, P.-J. Chen, M. Neupane, S.-Y. Xu, M. Z. Hasan, H. Lin, H.-T. Jeng, and A. Bansil, *Phys. Rev. B* **91**, 155151 (2015).
- [36] H. Weng, C. Fang, Z. Fang, B. A. Bernevig, and X. Dai, *Phys. Rev. X* **5**, 011029 (2015).
- [37] M. G. Zeng, C. Fang, G. Q. Chang, Y.-A. Chen, T. Hsieh, A. Bansil, H. Lin, and L. Fu, [arXiv:1504.03492](https://arxiv.org/abs/1504.03492).
- [38] P. Blaha, K. Schwarz, G. Madsen, D. Kvaniscka, and J. Luitz, *Wien2k, An Augmented Plane Wave Plus Local Orbitals Program for Calculating Crystal Properties* (Vienna University of Technology, Vienna, Austria, 2001).
- [39]  $d_{xy} \pm id_{x^2-y^2}$  and  $d_{xy}$  have the same  $C_{4z}$  eigenvalue. There is no difference in choosing either  $d_{xy}$  or  $d_{xy} \pm id_{x^2-y^2}$  as the basis vector.
- [40] S. Granville, B. J. Ruck, F. Budde, A. Koo, D. Pringle, F. Kuchler, A. Preston, D. Housden, N. Lund, A. Bittar, G. V. M. Williams, and H. J. Trodahl, *Phys. Rev. B* **73**, 235335 (2006).
- [41] H. J. Trodahl, A. R. H. Preston, J. Zhong, B. J. Ruck, N. M. Strickland, C. Mitra, and W. R. L. Lambrecht, *Phys. Rev. B* **76**, 085211 (2007).
- [42] H. Yoshitomi, S. Kitayama, T. Kita, O. Wada, M. Fujisawa, H. Ohta, and T. Sakurai, *Phys. Rev. B* **83**, 155202 (2011).
- [43] M. Schlipf, M. Betzinger, C. Friedrich, M. Ležaić, and S. Blügel, *Phys. Rev. B* **84**, 125142 (2011).
- [44] C.-G Duan, R. F. Sabiryanov, J. J. Liu, W. N. Mei, P. A. Dowben, and J. R. Hardy, *Phys. Rev. Lett.* **94**, 237201 (2005).
- [45] A. A. Mostofi, J. R. Yates, Y.-S. Lee, I. Souza, D. Vanderbilt, and N. Marzari, *Comput. Phys. Commun.* **178**, 685 (2008).
- [46] See Supplemental Material at <http://link.aps.org/supplemental/10.1103/PhysRevB.92.201303> for the calculated band structures and surface states of GdN.